第 22 卷第 5 期
2024 年 5 月

动力学与控制学报
JOURNAL OF DYNAMICS AND CONTROL

Vol. 22 No. 5
May 2024

文章编号:1672-6553-2024-22(5)-008-008　　DOI:10.6052/1672-6553-2023-059

限幅型非光滑吸振器模型的稳定性与周期运动研究*

郭子玉[1,2]　李静[1†]　朱绍涛[1,3]　张伟[1,4]

(1. 北京工业大学 数学统计学与力学学院,北京　100124)
(2. 清华大学 材料学院,北京　100084)
(3. 北京工业大学 信息学部,北京　100124)
(4. 广西大学 土木建筑工程学院,南宁　530004)

摘要　本文研究具有分段光滑特性的限幅型吸振器模型的稳定性与周期运动. 建立一类限幅型非光滑吸振器的动力学模型,探讨模型容许平衡点的存在性,通过 Liénard-Chipart 稳定性准则,分析容许平衡点的稳定性. 通过参数变换,将限幅型吸振器模型转化为具有两个切换流形的四维分段光滑系统. 通过计算系统首次积分,获得四维含参分段光滑动力系统在其未扰系统存在一族周期轨条件下的 Melnikov 函数. 探讨不同参数条件下系统周期轨的存在性及个数,并利用数值模拟方法给出其相图构型,验证理论结果的正确性. 研究结果表明不同的间隙参数影响系统周期轨个数及相对位置.

关键词　非光滑吸振器，　高维分段光滑系统，　稳定性，　周期运动，　Melnikov 方法

中图分类号:O322　　**文献标志码**:A

Stability and Periodic Motions for a Non-Smooth Vibration Absorber Model with Limited Amplitude*

Guo Ziyu[1,2]　Li Jing[1†]　Zhu Shaotao[1,3]　Zhang Wei[1,4]

(1. School of Mathematics, Statistics and Mechanics, Beijing University of Technology, Beijing　100124, China)
(2. School of Materials Science and Engineering, Tsinghua University, Beijing　100084, China)
(3. Faculty of Information Technology, Beijing University of Technology, Beijing　100124, China)
(4. School of Civil Engineering and Architecture, Guangxi University, Nanning　530004, China)

Abstract　In this paper, the stability and periodic motions for a limited vibration absorber model with the piecewise smooth property are studied. The dynamic model of a kind of limited vibration absorber is established. The existence of the admissible equilibrium point of the model is discussed, and the stability of the admissible equilibrium point is analyzed by Liénard-Chipart stability criterion. With the aid of parameter transformations, the vibration absorber model with limited amplitude is transformed into a four-dimensional piecewise smooth system with two switching manifolds. By the first integrals of the system, the Melnikov function of the four-dimensional parametric piecewise smooth dynamic system under the condition that the unperturbed system has a family of periodic orbits is obtained. The existence and number of periodic orbits of the system under different parameter conditions are discussed, and the phase diagram configuration is given by numerical simulation method to verify the correctness of the theoretical results. The results show that different clearance parameters affect the number and relative positions of

2023-04-21 收到第 1 稿,2023-05-22 收到修改稿.

* 国家自然科学基金资助项目(12272011), 国家重点研发计划(2022YFB3806000), National Natural Science Foundation of China (12272011), National Key R&D Program of China (2022YFB3806000).

† 通信作者 E-mail:leejing@bjut.edu.cn

periodic orbits.

Key words　non-smooth vibration absorber,　high-dimensional piecewise smooth systems,　stability,　periodic motions,　Melnikov method

引言

动力吸振器(Dynamic vibration absorber)概念由 Frahm[1] 率先提出,Den Hartog[2] 与 Hunt[3] 等专家学者在此基础上发展了诸多创新成果,广泛应用于实际工程中的振动控制. 复杂工况环境下的振动是影响工程结构运行高效性、可靠性、准确性与安全性的重要因素,对复杂动力学环境中的有害振动进行抑制,是重大工程领域的技术难题与前沿课题[4,5].

不同学者针对非光滑吸振器进行型式设计,并研究具有分段刚度或分段阻尼特性的非光滑吸振器[6-9] 和碰撞振动非光滑吸振器[10,11] 等多种模型. 胡海岩和金栋平[6] 提出了一种刚度分段线性变化的动力吸振器,并研究其半主动控制策略. Chen 等[7] 研制了一种刚度递减的分段式非线性能量汇(Nonlinear energy sink, NES),并分析了该模型对稳定高分支响应的抑制效果. Li 等[8] 通过数值模拟研究了分段线性 NES 的能量俘获和靶向能量传递. Geng 和 Ding 等[9] 提出了一种具有接地分段刚度的限幅型 NES,考虑了瞬态响应下分段刚度和间隙对 NES 和主结构振动响应的影响. Fang 等[10] 将碰撞振动非光滑吸振器应用于对悬臂梁的振动抑制,研究表明使用多个碰撞振动非光滑吸振器能够有效地拓宽振动抑制的频率范围. Qiu 等[11] 研究了碰撞振动式 NES 耦合线性振子结构的靶向能量传递效率和分岔现象,并将所得结果推广到多个碰撞振动 NES 的应用中.

研究吸振器模型的稳定性与周期运动等复杂动力学行为对于揭示吸振器的振动控制机制及能量传递机理至关重要. Lee 等[12] 研究发现理解无阻尼系统的周期动力学为解释有阻尼系统瞬态动力学中的能量传递现象和不同类型运动之间的复杂转换提供指导. Al-Shudeifat 和 Saeed[13] 研究了附着分段 NES 的两自由度结构的周期运动与频—能曲线,进一步增加对 NES 能量靶向传递的理解. Wang 等[14] 研究了 Van der Pol 振子与 NES 耦合系统在低频受迫激励下的动力学行为,并分析其减振机理. Lelkes 等[15] 针对分段线性气动弹性系统分别在有、无调谐吸振器情形下分析系统的稳定性及平衡点分岔问题. Li 等[16] 研究了压电俘能器集成的非线性能量汇在简谐激励下的动力学与评估. Li 等[17] 发展了一类具有双边刚性约束平面非光滑系统的 Melnikov 方法,应用于研究一类新型碰撞振动双稳态 NES 的全局动力学. Wang 等[18] 研究了一类分段线性系统耦合 NES 的减振问题,采用谐波平衡法分析耦合系统的稳态响应.

具有非光滑特性的吸振器与主振子系统的耦合模型可由高维非光滑系统描述,其周期解分岔的研究是非线性动力学领域的前沿课题[19]. Melnikov 方法是研究非光滑系统的有效工具之一,李双宝等[20] 综述了适用于研究非光滑系统全局动力学 Melnikov 方法的相关进展. 针对高维非光滑系统周期运动问题,Luo 和 Xie 等[21] 研究了一类两自由度碰撞系统的周期运动与全局分岔问题. Granados 等[22] 通过 scattering 映射与 Melnikov 方法研究了一类 4 维耦合非自治分段光滑系统在异宿轨附近的动力学特性,并应用于碰撞机械系统. Guo 和 Tian 等[23] 研究一类高维非光滑耦合系统的次谐 Melnikov 函数. Li 等[24] 研究一类具有两个切换流形的高维分段光滑近可积系统的周期解分岔问题,并给出其 Melnikov 向量函数的具体表达式.

针对非光滑吸振器与主振子耦合结构的动力学行为,已有学者分析准周期运动与分岔行为同能量传递之间的作用机理,但对系统稳定性及存在复杂多周期运动现象的内在机理还不是十分清楚,需要基于高维非光滑系统的稳定性及周期解理论开展深入研究. 本文研究两自由度限幅型非光滑吸振器模型的稳定性及周期运动. 以间隙和刚度等为主要参数,探讨其对系统稳定性及周期运动的影响,研究系统周期轨道的存在性、个数及相对位置. 借助数值模拟,给出系统周期轨道的相图构型.

1　非光滑吸振器模型

本节考虑一类具有分段特性的限幅型非光滑

吸振器模型. 根据文献[9]非线性能量汇模型,建立如图1所示的非光滑吸振器模型.

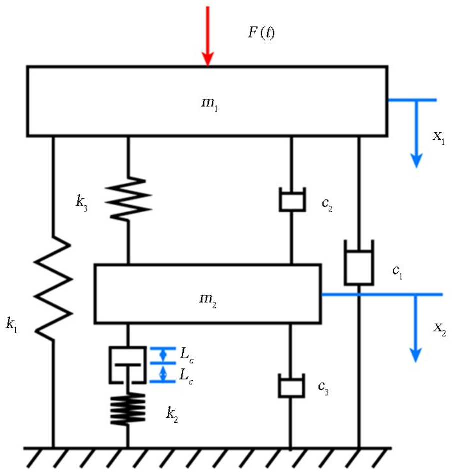

图1 非光滑吸振器模型

Fig. 1 The non-smooth vibration absorber model

耦合非光滑吸振器线性振子的运动常微分方程如下所示

$$m_1\ddot{x}_1+c_1\dot{x}_1+k_1x_1=F(t)+c_2(\dot{x}_2-\dot{x}_1)+k_3(x_2-x_1)\tag{1a}$$

$$m_2\ddot{x}_2+c_2(\dot{x}_2-\dot{x}_1)+k_3(x_2-x_1)+g(x_2)+c_3\dot{x}_2=0\tag{1b}$$

其中"·"表示 d/dt,x_1、x_2 和 m_1、m_2 分别为主振子和吸振器的位移和质量,c_1、c_2、c_3 为阻尼系数,k_1、k_2 和 k_3 为刚度系数. 外激励项为 $F(t)=a\cos(\omega t)$,L_c 为间隙距离,则分段恢复力为

$$g(x_2)=\begin{cases}k_2(x_2-L_c), & x_2>L_c\\ 0, & -L_c\leqslant x_2\leqslant L_c\\ k_2(x_2+L_c), & x_2<-L_c\end{cases}$$

系统(1a)、系统(1b)的无量纲方程为

$$\ddot{\bar{x}}_2=-\tilde{g}(\bar{x}_2)-u_1(\bar{x}_2-\bar{x}_1)-(2\zeta_1+2\zeta_2)\dot{\bar{x}}_2+2\zeta_1\dot{\bar{x}}_1\tag{2a}$$

$$\ddot{\bar{x}}_1=\rho u_1\bar{x}_2+2\zeta_4\dot{\bar{x}}_2-(\rho u_2+\rho u_1)\bar{x}_1-(2\zeta_3+2\zeta_4)\dot{\bar{x}}_1+w\tag{2b}$$

其中 $\bar{t}=\omega_1 t$,为方便书写,去除无量纲参数 $\bar{t}$ 上标,

$$\bar{x}_1=\frac{x_1}{D},\bar{x}_2=\frac{x_2}{D},L=\frac{L_c}{D},\rho=\frac{m_2}{m_1},\omega_1=\sqrt{\frac{k_2}{m_2}},$$

$$\omega_2=\sqrt{\frac{k_1}{m_1}},\zeta_1=\frac{c_2}{2m_2\omega_1},\zeta_2=\frac{c_3}{2m_2\omega_1},\zeta_3=\frac{c_1}{2m_1\omega_1},$$

$$\zeta_4=\frac{c_2}{2m_1\omega_1},u_1=\frac{k_3}{k_2},u_2=\frac{k_1}{k_2},w=\frac{a}{D\omega_1^2}\cos\frac{\omega}{\omega_1}\bar{t},$$

$$\tilde{g}(\bar{x}_2)=\begin{cases}\bar{x}_2-L, & \bar{x}_2>L\\ 0, & -L\leqslant\bar{x}_2\leqslant L.\\ \bar{x}_2+L, & \bar{x}_2<-L\end{cases}$$

根据文献[25],当外激励频率 ω 远远小于固有频率时,可以将 w 视为一个慢变参数,称系统(2)为广义自治系统. 探讨该广义自治系统的平衡点稳定性及周期解分岔问题.

2 平衡点与稳定性分析

引入状态向量 $\boldsymbol{x}=(\bar{x}_2,\dot{\bar{x}}_2,\bar{x}_1,\dot{\bar{x}}_1)^{\mathrm{T}}$,定义系统的切换流形为

$$\boldsymbol{\Pi}^+=\{\boldsymbol{x}\in\mathbf{R}^4\mid\bar{x}_2=L\},$$

$$\boldsymbol{\Pi}^-=\{\boldsymbol{x}\in\mathbf{R}^4\mid\bar{x}_2=-L\}.$$

由两个切换流形分割的三个区域

$$D_{\mathrm{r}}=\{\boldsymbol{x}\in\mathbf{R}^4\mid\bar{x}_2>L\},$$

$$D_{\mathrm{c}}=\{\boldsymbol{x}\in\mathbf{R}^4\mid -L<\bar{x}_2<L\},$$

$$D_{\mathrm{l}}=\{\boldsymbol{x}\in\mathbf{R}^4\mid\bar{x}_2<-L\}.$$

定义在 $D_i(i=r,c,l)$ 上的子系统分别为

$$\dot{\boldsymbol{x}}=\boldsymbol{f}^{\mathrm{r}}(\boldsymbol{x})=\boldsymbol{A}_{\mathrm{r}}\boldsymbol{x}+\boldsymbol{b}_{\mathrm{r}},\ \boldsymbol{x}\in D_{\mathrm{r}}\tag{3a}$$

$$\dot{\boldsymbol{x}}=\boldsymbol{f}^{\mathrm{c}}(\boldsymbol{x})=\boldsymbol{A}_{\mathrm{c}}\boldsymbol{x}+\boldsymbol{b}_{\mathrm{c}},\ \boldsymbol{x}\in D_{\mathrm{c}}\cup\boldsymbol{\Pi}^+\cup\boldsymbol{\Pi}^-\tag{3b}$$

$$\dot{\boldsymbol{x}}=\boldsymbol{f}^{\mathrm{l}}(\boldsymbol{x})=\boldsymbol{A}_l\mathbf{x}+\boldsymbol{b}_{\mathrm{l}},\ \boldsymbol{x}\in D_{\mathrm{l}}\tag{3c}$$

其中

$$\begin{aligned}\boldsymbol{A}_r=\boldsymbol{A}_1=&\partial_{1,2}^{4;4}(1)+\partial_{2,1}^{4;4}(-1-u_1)+\partial_{2,3}^{4;4}(u_1)+\partial_{2,2}^{4;4}(-2\zeta_1-2\zeta_2)+\partial_{2,4}^{4;4}(2\zeta_1)+\\&\partial_{3,4}^{4;4}(1)+\partial_{4,1}^{4;4}(\rho u_1)+\partial_{4,2}^{4;4}(2\zeta_4)+\partial_{4,3}^{4;4}(-\rho u_1-\rho u_2)+\partial_{4,4}^{4;4}(-2\zeta_3-2\zeta_4),\end{aligned}$$

$$\begin{aligned}\boldsymbol{A}_{\mathrm{c}}=&\partial_{1,2}^{4;4}(1)+\partial_{2,1}^{4;4}(-u_1)+\partial_{2,3}^{4;4}(u_1)+\partial_{2,2}^{4;4}(-2\zeta_1-2\zeta_2)+\partial_{2,4}^{4;4}(2\zeta_1)+\partial_{3,4}^{4;4}(1)+\\&\partial_{4,1}^{4;4}(\rho u_1)+\partial_{4,2}^{4;4}(2\zeta_4)+\partial_{4,3}^{4;4}(-\rho u_1-\rho u_2)+\partial_{4,4}^{4;4}(-2\zeta_3-2\zeta_4),\end{aligned}$$

$$\boldsymbol{b}_{\mathrm{r}}=\partial_{2,1}^{4;1}(L)+\partial_{4,1}^{4;1}(w),$$

$$\boldsymbol{b}_{\mathrm{c}}=\partial_{4,1}^{4;1}(w),$$

$$\boldsymbol{b}_{\mathrm{l}}=\partial_{2,1}^{4;1}(-L)+\partial_{4,1}^{4;1}(w).$$

$\partial_{p,q}^{m;n}(\boldsymbol{M})$ 为第(p,q)阶分块矩阵为$\boldsymbol{M}$其余部分为0的 $m\times n$ 矩阵[26]. 根据文献[19],可得如下定义.

定义1 称平衡点为容许平衡点(admissible equilibrium point)若满足$(\dot{\boldsymbol{x}}^*)=\boldsymbol{f}^i(\boldsymbol{x}^*)$且$\boldsymbol{x}^*\in D_i$. 若满足$(\dot{\boldsymbol{x}}^*)=\boldsymbol{f}^i(\dot{\boldsymbol{x}}^*)$,$\dot{\boldsymbol{x}}^*\in D_j$ 且 $i\neq j$,则称该平衡点为虚拟平衡点(virtual equilibrium point).

由系统(3a)~(3c)可得平衡点为

$$\boldsymbol{E}_{\mathrm{c}}=\frac{w}{\rho u_2}\left[\partial_{1,1}^{4;1}(1)+\partial_{3,1}^{4;1}(1)\right],\ \boldsymbol{x}\in D_c\cup\boldsymbol{\Pi}^+\cup\boldsymbol{\Pi}^-\tag{4a}$$

$$\boldsymbol{E}_r = \partial_{1,1}^{4,1}\left[\frac{(u_1+u_2)L\rho + u_1 w}{\rho(u_1u_2+u_1+u_2)}\right] + \partial_{3,1}^{4,1}\left[\frac{u_1L\rho+(1+u_1)w}{\rho(u_1u_2+u_1+u_2)}\right],\quad x\in D_r \tag{4b}$$

$$\boldsymbol{E}_l = \partial_{1,1}^{4,1}\left[\frac{u_1 w-(u_1+u_2)L\rho}{\rho(u_1u_2+u_1+u_2)}\right] + \partial_{3,1}^{4,1}\left[\frac{(1+u_1)w-u_1L\rho}{\rho(u_1u_2+u_1+u_2)}\right],\quad x\in D_l \tag{4c}$$

根据定义 1,分别讨论平衡点为容许平衡点 $\boldsymbol{E}_c$,$\boldsymbol{E}_r$,$\boldsymbol{E}_l$ 的参数范围.

若 $-L\leqslant\dfrac{w}{\rho u_2}\leqslant L$,$\boldsymbol{E}_c$ 是容许平衡点;

若 $\dfrac{(u_1+u_2)L\rho+u_1w}{\rho(u_1u_2+u_1+u_2)}>L$,$\boldsymbol{E}_r$ 是容许平衡点;

若 $\dfrac{u_1w-(u_1+u_2)L\rho}{\rho(u_1u_2+u_1+u_2)}<-L$,$\boldsymbol{E}_l$ 是容许平衡点.

讨论 $\boldsymbol{E}_c$ 在满足 $-L\leqslant\dfrac{w}{\rho u_2}\leqslant L$ 条件的稳定性,由(3b)可得其特征方程为

$$\lambda^4+a_1\lambda^3+a_2\lambda^2+a_3\lambda+a_4=0 \tag{5}$$

其中

$$a_1=2\zeta_3+2\zeta_4+2\zeta_2+2\zeta_1,$$
$$a_2=\rho u_1+\rho u_2+4\zeta_1\zeta_3+4\zeta_2\zeta_3+4\zeta_2\zeta_4+u_1,$$
$$a_3=2\rho u_1\zeta_2+2\rho u_2\zeta_1+2\rho u_2\zeta_2+2u_1\zeta_3,$$
$$a_4=2\rho u_1u_2,\boldsymbol{\Delta}_1=a_1,$$
$$\boldsymbol{\Delta}_3=\begin{vmatrix} a_1 & a_3 & 0\\ 1 & a_2 & a_4\\ 0 & a_1 & a_3\end{vmatrix}.$$

根据 Liénard-Chipart 稳定性准则[15]可知,方程(5)所有根都有负实部的充要条件为

$$a_2>0,\quad a_4>0,$$
$$\boldsymbol{\Delta}_1=a_1>0,\quad \boldsymbol{\Delta}_3>0 \tag{6}$$

在参数条件为

$$P_{ar1}=(\rho,u_2,\zeta_1,\zeta_2,\zeta_3,\zeta_4,w,L)=(0.1,6,0.2,0.01,0.05,0.2,0.1,1).$$

由(6)可得图 2.

图 2 的纵坐标为 a_1、a_2、a_4 和 $\boldsymbol{\Delta}_3$ 的值. 由 $\boldsymbol{\Delta}_3=0$ 可解得 u_{11},u_{12},由图 2 与稳定性条件可知,$\boldsymbol{E}_c$ 在参数条件 P_{ar1} 一直是容许平衡点,在区间 $(0,u_{11})\cup(u_{12},+\infty)$ 为渐进稳定的,在区间 $[u_{11},u_{12}]$ 为不稳定的.

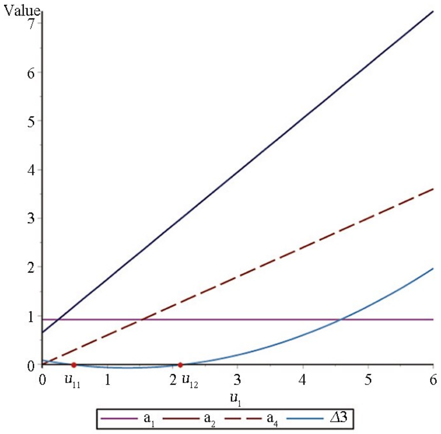

图 2　a_1、a_2、a_4 和 $\boldsymbol{\Delta}_3$ 表达式

Fig. 2　The expression of a_1、a_2、a_4 and $\boldsymbol{\Delta}_3$

由稳定性条件可知,当外激励频率与固有频率存在量级差时,w 不影响系统稳定性. 分别探讨在渐近稳定与不稳定区域,当 $F(t)=0.5\cos(0.01t)$ 时,非光滑吸振器的吸振效果.

情形 1:$u_1=1$.

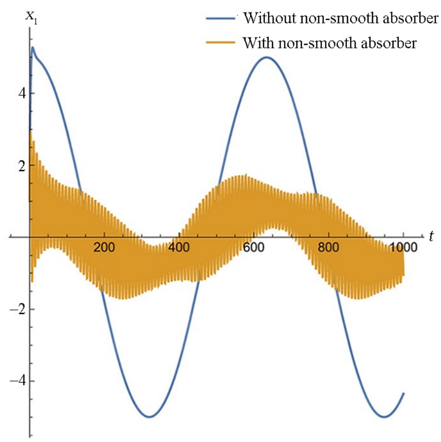

图 3　系统(1)在 $u_1=1$ 条件下有无非光滑吸振器时主系统时间历程图

Fig. 3　The time history diagram of the main system (1) with and without non-smooth vibration absorber under $u_1=1$

情形 2:$u_1=3$.

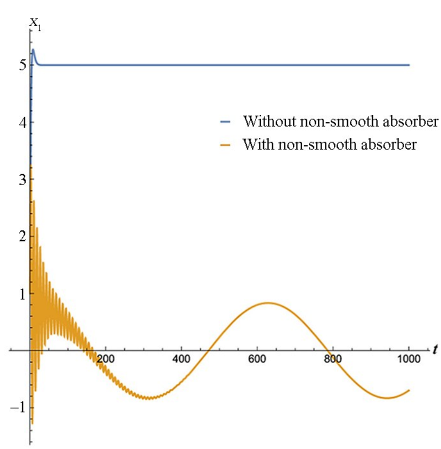

图 4　系统(1)在 $u_1=3$ 有无非光滑吸振器时主系统时间历程图

Fig. 4　The time history diagram of the main system (1) with and without non-smooth vibration absorber under $u_1=3$

图3和图4表明该类限幅型非光滑吸振器在 $u_1=1$ 和 $u_1=3$ 条件能够有效地降低主系统振幅.

3 周期轨分岔与数值模拟

将系统(2)变换为如下形式

$$\ddot{\bar{x}}_2=-\tilde{g}(\bar{x}_2)-p_1(\bar{x}_2-\bar{x}_1)-p_2\dot{\bar{x}}_2+p_3\dot{\bar{x}}_1 \tag{7a}$$

$$\ddot{\bar{x}}_1=e_1(\bar{x}_2-\bar{x}_1)+e_2\dot{\bar{x}}_2-e_3\bar{x}_1-e_4\dot{\bar{x}}_1+e_5 \tag{7b}$$

其中

$p_1=u_1, p_2=(2\zeta_1+2\zeta_2), p_3=2\zeta_1$,

$e_1=\rho u_1, e_2=2\zeta_4, e_3=\rho u_2$,

$e_4=2\zeta_3+2\zeta_4, e_5=w$.

引入扰动变换 $p_k\to\varepsilon p_k, e_l\to\varepsilon^2 e_l, e_4\to\varepsilon e_4$, $k=1,2, l=1,2,3,5$ 系统(7a)和系统(7b)可化为

$$\ddot{\bar{x}}_2=-\tilde{g}(\bar{x}_2)+\varepsilon[-p_1(\bar{x}_2-\bar{x}_1)-p_2\dot{\bar{x}}_2]+p_3\dot{\bar{x}}_1 \tag{8a}$$

$$\ddot{\bar{x}}_1=\varepsilon^2[e_1(\bar{x}_2-\bar{x}_1)+e_2\dot{\bar{x}}_2-e_3\bar{x}_1+e_5]-\varepsilon e_4\dot{\bar{x}}_1 \tag{8b}$$

令 $\dot{\bar{x}}_2=w_1, \dot{\bar{x}}_1=\varepsilon w_2, y_1=\bar{x}_2, y_2=w_1, y_3=\bar{x}_1, y_4=w_2$,系统(8a)和系统(8b)可化为

$$\begin{aligned}
\dot{y}_1&=y_2\\
\dot{y}_2&=-\dot{g}(y_1)+\varepsilon[-p_1(y_1-y_3)-p_2y_2+p_3y_4]\\
\dot{y}_3&=\varepsilon y_4\\
\dot{y}_4&=\varepsilon[e_1(y_1-y_3)+e_2y_2-e_3y_3-e_4y_4+e_5]
\end{aligned} \tag{9}$$

其中

$$\dot{g}(y_1)=\begin{cases}y_1-L, & y_1>L\\ 0, & -L\leqslant y_1\leqslant L\\ y_1+L, & y_1<-L\end{cases}.$$

其未扰子系统的首次积分分别为

$$\boldsymbol{H}^{r}=[\frac{1}{2}y_2^2+\frac{1}{2}(y_1-L)^2, y_3, y_4],$$

$$\boldsymbol{H}^{c}=(\frac{1}{2}y_2^2, y_3, y_4),$$

$$\boldsymbol{H}^{l}=[\frac{1}{2}y_2^2+\frac{1}{2}(y_1+L)^2, y_3, y_4].$$

讨论当 $h_1>0$ 情况下系统的周期轨分岔问题,可得其轨线 $\boldsymbol{\Gamma}^s_{h_1,\hat{h}}(s=1,\cdots,4)$ 为

$\boldsymbol{\Gamma}^1_{h_1,\hat{h}}: y_1=\sqrt{2h_1-y_2^2}+L, -\sqrt{2h_1}\leqslant y_2\leqslant\sqrt{2h_1}$,

$\boldsymbol{\Gamma}^2_{h_1,\hat{h}}: y_2=-\sqrt{2h_1}, -L\leqslant y_1\leqslant L$,

$\boldsymbol{\Gamma}^3_{h_1,\hat{h}}: y_1=-\sqrt{2h_1-y_2^2}-L, -\sqrt{2h_1}\leqslant y_2\leqslant\sqrt{2h_1}$,

$\boldsymbol{\Gamma}^4_{h_1,\hat{h}}: y_2=\sqrt{2h_1}, -L\leqslant y_1\leqslant L$.

交点坐标分别为

$A_1^*=(L,\sqrt{2h_1}), A_2^*=(L,-\sqrt{2h_1})$,

$A_3^*=(-L,-\sqrt{2h_1}), A_4^*=(-L,\sqrt{2h_1})$.

应用文献[24]定理2,其首阶Melnikov函数为

$$M_1(h)=4h_1p_2\sin(\theta)\cos(\theta)+4h_1p_2\theta+4\sqrt{2h_1}Lp_1L\sin(\theta)-4\sqrt{2h_1}p_2L, \tag{10a}$$

$$M_2(h)=2h_3\pi+\frac{2\sqrt{2}h_3L}{\sqrt{h_1}}, \tag{10b}$$

$$M_3(h)=-\frac{2}{\sqrt{h_1}}(\sqrt{2}e_1Lh_2+\sqrt{2}e_3Lh_2+\sqrt{2}Le_4h_3+\sqrt{h_1}\pi e_1h_2+e_3\pi h_2\sqrt{h_1}+e_4\pi\sqrt{h_1}h_3-\sqrt{2}Le_5-\pi\sqrt{h_1}e_5) \tag{10c}$$

其中 $\theta=\arcsin\frac{\sqrt{2h_1}}{\sqrt{L^2+2h_1}}, \sin\theta=\frac{\sqrt{2h_1}}{\sqrt{L^2+2h_1}}, \cos\theta=\frac{L}{\sqrt{L^2+2h_1}}$.

由 $M_2(h_1)=0, M_3(h)=0$ 可得 $h_2=\frac{e_5}{e_1+e_3}, h_3=0$. 因此,系统(9)周期轨道个数及分岔问题取决于 M_1 零解的个数. 讨论当参数满足如下条件周期轨的个数问题.

$$\begin{aligned}P_{ar2}&=(p_1,p_3,e_1,e_2,e_3,e_4,e_5)\\&=(0.5,1,0.2,1,0.5,2,0.01).\end{aligned}$$

由 $M_1(h)=0$ 可得 p_2, L, h_1 关系如图5所示.

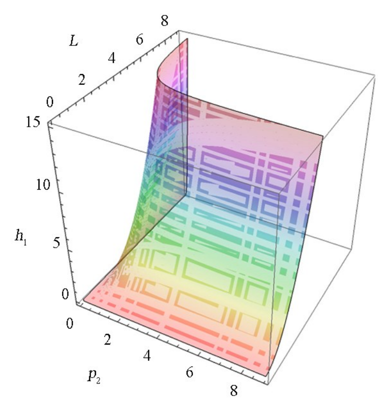

图5 系统(9)的关系图

Fig. 5 The relationship between of system (9)

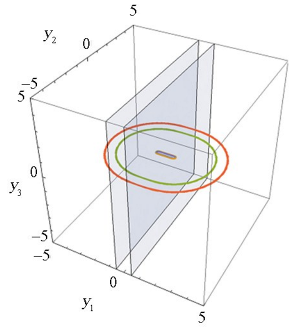

(a) 在空间 (y_1,y_2,y_3) 投影
(a) Projection in space (y_1,y_2,y_3)

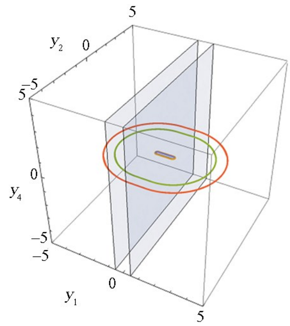

(b) 在空间 (y_1,y_2,y_4) 投影
(b) Projection in space (y_1,y_2,y_4)

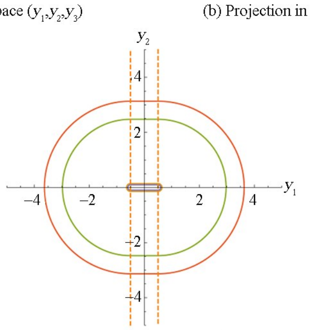

(c) 在平面(y_1,y_2) 投影
(c)Projection in plane(y_1,y_2)

图 6　在$(p_2,L)=(0.1,0.5)$时系统(9)周期轨
Fig. 6　Periodic orbits of system (9) under $(p_2,L)=(0.1,0.5)$

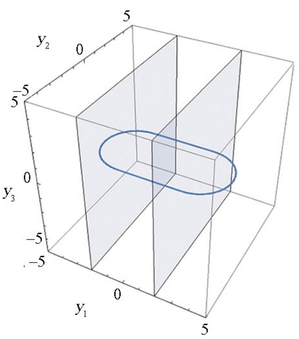

(a) 在空间 (y_1,y_2,y_3) 投影
(a) Projection in space (y_1,y_2,y_3)

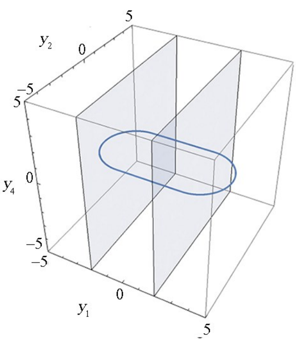

(b) 在空间 (y_1,y_2,y_4) 投影
(b) Projection in space (y_1,y_2,y_4)

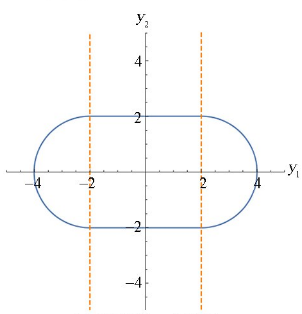

(c) 在平面(y_1,y_2) 投影
(c)Projection in plane(y_1,y_2)

图 7　在$(p_2,L)=(1,2)$时系统(9)周期轨
Fig. 7　A periodic orbit of system (9) under $(p_2,L)=(1,2)$

图 5 中曲面为 $M_1(h)=0$ 三维等值面，可得在(p_2,L)取不同值时对应 h_1 的情况，即系统(9)解的个数情况．由式(7)可知，p_2 为与系统阻尼 c_2 和 c_3 相关的参数，L 为间隙参数．以下讨论在(p_2,L)取不同值情形下广义自治系统周期解的个数．

当$(p_2,L)=(0.1,0.5)$，方程(10a)有 5 个实根，且在解处的 Jacobi 矩阵行列式不为零，则系统(9)周期轨分别在空间(y_1,y_2,y_3)、(y_1,y_2,y_4)与平面(y_1,y_2)的投影如图 6(a)～图 6(c)所示．

当$(p_2,L)=(1,2)$，方程(10a)有 1 个实根，且在解处的 Jacobi 矩阵行列式不为零，则系统(9)周期轨分别在空间(y_1,y_2,y_3)、(y_1,y_2,y_4)与平面(y_1,y_2)的投影如图 7(a)～图 7(c)所示．

当$(p_2,L)=(0.3,0.5)$，方程(10a)有 3 个实根，且在解处的 Jacobi 矩阵行列式不为零，则系统(9)周期轨分别在空间(y_1,y_2,y_3)、(y_1,y_2,y_4)与平面(y_1,y_2)的投影如图 8(a)～图 8(c)所示．

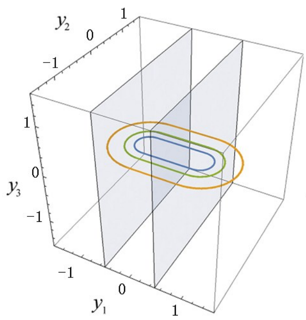

(a) 在空间(y_1,y_2,y_3)投影
(a) Projection in space (y_1,y_2,y_3)

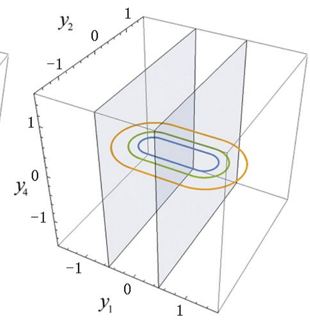

(b)在空间(y_1,y_2,y_4)投影
(b) Projection in space (y_1,y_2,y_4)

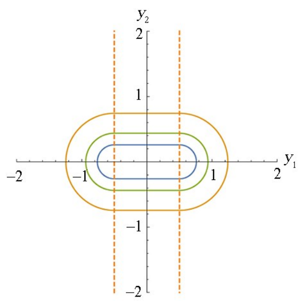

(c) 在平面(y_1,y_2) 投影
(c)Projection in plane(y_1,y_2)

图 8　在$(p_2,L)=(0.3,0.5)$时系统(9)周期轨
Fig. 8　Periodic orbits of system (9) under $(p_2,L)=(0.3,0.5)$

4　结论

非光滑吸振器稳定性及周期运动的研究对分析其能量传递与振动控制具有重要理论意义．本文获得具有分段特性限幅型吸振器模型容许平衡点的存在性条件，通过 Liénard-Chipart 稳定性准则，分别探讨刚度比对容许平衡点稳定性的影响并给出其渐进稳定与不稳定参数范围．

针对 4 维具有分段特性的限幅型吸振器模型，通过首次积分，计算其在未扰存在一族周期轨条件下的 Melnikov 函数，获得 p_2,L,h_1 的关系图．分

别探讨在不同参数条件下周期轨的存在性及个数问题. 在(p_2,L)=(0.1,0.5)时,系统存在 5 个周期轨;在(p_2,L)=(1,2)时,系统存在 1 个周期轨;在(p_2,L)=(0.3,0.5)时,系统存在 3 个周期轨. 基于数值模拟,针对其几何构型给出描述. 该结果丰富了高维分段光滑系统周期运动的研究,为非光滑吸振器模型的减振控制与结构设计提供理论指导.

参考文献

[1] HERMANN F. Device for damping vibrations of bodies: US0989958 [P]. 1911-04-18.

[2] DEN HARTOG J P. Mechanical vibrations [M]. 4th ed. New York: McGraw-Hill, 1956.

[3] HUNT J B. Dynamic vibration absorbers [M]. London: Mechanical Engineering Publications, 1979.

[4] 徐鉴. 振动控制研究进展综述[J]. 力学季刊, 2015, 36(4): 547-565.
XU J. Advances of research on vibration control [J]. Chinese Quarterly of Mechanics, 2015, 36(4): 547-565. (in Chinese)

[5] ZHOU J X, DOU L L, WANG K, et al. A nonlinear resonator with inertial amplification for very low-frequency flexural wave attenuations in beams [J]. Nonlinear Dynamics, 2019, 96(1): 647-665.

[6] 胡海岩, 金栋平. 基于分段线性吸振器的振动半主动控制[J]. 振动工程学报, 1997, 10(2): 125-130.
HU H Y, JIN D P. A semi-active vibration control strategy based on piecewise-linear vibration absorber [J]. Journal of Vibration Engineering, 1997, 10(2): 125-130. (in Chinese)

[7] CHEN J E, SUN M, HU W H, et al. Performance of non-smooth nonlinear energy sink with descending stiffness [J]. Nonlinear Dynamics, 2020, 100(1): 255-267.

[8] LI X L, LIU K F, XIONG L Y, et al. Development and validation of a piecewise linear nonlinear energy sink for vibration suppression and energy harvesting [J]. Journal of Sound and Vibration, 2021, 503: 116104.

[9] GENG X F, DING H, MAO X Y, et al. Nonlinear energy sink with limited vibration amplitude [J]. Mechanical Systems and Signal Processing, 2021, 156: 107625.

[10] FANG B, THEURICH T, KRACK M, et al. Vibration suppression and modal energy transfers in a linear beam with attached vibro-impact nonlinear energy sinks [J]. Communications in Nonlinear Science and Numerical Simulation, 2020, 91: 105415.

[11] QIU D, SEGUY S, PAREDES M. Design criteria for optimally tuned vibro-impact nonlinear energy sink [J]. Journal of Sound and Vibration, 2019, 442: 497-513.

[12] LEE Y S, KERSCHEN G, VAKAKIS A F, et al. Complicated dynamics of a linear oscillator with a light, essentially nonlinear attachment [J]. Physica D: Nonlinear Phenomena, 2005, 204(1/2): 41-69.

[13] AL-SHUDEIFAT M A, SAEED A S. Periodic motion and frequency energy plots of dynamical systems coupled with piecewise nonlinear energy sink [J]. Journal of Computational and Nonlinear Dynamics, 2022, 17(4): 041005.

[14] WANG Y L, LI X H, SHEN Y J. Vibration reduction mechanism of Van der Pol oscillator under low-frequency forced excitation by means of nonlinear energy sink [J]. International Journal of Non-Linear Mechanics, 2023, 152: 104389.

[15] LELKES J, KALMAR-NAGY T. Analysis of a piecewise linear aeroelastic system with and without tuned vibration absorber [J]. Nonlinear Dynamics, 2021, 103(4): 2997-3018.

[16] LI X, ZHANG Y W, DING H, et al. Dynamics and evaluation of a nonlinear energy sink integrated by a piezoelectric energy harvester under a harmonic excitation [J]. Journal of Vibration and Control, 2019, 25(4): 851-867.

[17] LI S B, ZHOU X X, CHEN J E. Hamiltonian dynamics and targeted energy transfer of a grounded bistable nonlinear energy sink [J]. Communications in Nonlinear Science and Numerical Simulation, 2023, 117: 106898.

[18] WANG X, GENE X F, MAO X Y, et al. Theoretical and experimental analysis of vibration reduction for piecewise linear system by nonlinear energy sink [J]. Mechanical Systems and Signal Processing, 2022, 172: 109001.

[19] DI BERNARDO M, BUDD CJ, CHAMPNEYS A R, et al. Piecewise-smooth dynamical systems:

theory and applications [M]. London: Springer, 2008.

[20] 李双宝，马茜茜，张伟. 非光滑系统全局动力学Melnikov方法的研究进展[J]. 动力学与控制学报，2020，18(2)：9−20.
LI S B, MA X X, ZHANG W. Research progress in Melnikov method for global dynamics of non-smooth systems [J]. Journal of Dynamics and Control, 2020, 18(2): 9−20. (in Chinese)

[21] LUO G W, XIE J H, GUO S H L. Periodic motions and global bifurcations of a two-degree-of-freedom system with plastic vibro-impact [J]. Journal of Sound and Vibration, 2001, 240(5): 837−858.

[22] GRANADOS A, HOGAN S J, SEARA T M. The scattering map in two coupled piecewise-smooth systems, with numerical application to rocking blocks [J]. Physica D: Nonlinear Phenomena, 2014, 269: 1−20.

[23] GUO X Y, TIAN R L, XUE Q, et al. Sub-harmonic Melnikov function for a high-dimensional non-smooth coupled system [J]. Chaos, Solitons & Fractals, 2022, 164: 112629.

[24] LI J, GUO Z Y, ZHU S T, et al. Bifurcation of periodic orbits and its application for high-dimensional piecewise smooth near integrable systems with two switching manifolds [J]. Communications in Nonlinear Science and Numerical Simulation, 2023, 116: 106840.

[25] 张晓芳，吴磊，毕勤胜. 周期激励下四维非线性系统的簇发共存现象[J]. 动力学与控制学报，2016，14(5)：422−428.
ZHANG X F, WU L, BI Q S. Bursting coexistence phenomenon of a four-dimensional non-autonomous system under periodic excitation [J]. Journal of Dynamics and Control, 2016, 14(5): 422−428. (in Chinese)

[26] LI J, ZHANG L N, WANG D. Unique normal form of a class of 3 dimensional vector fields with symmetries [J]. Journal of Differential Equations, 2014, 257(7): 2341−2359.